JOURNAL OF SOLID STATE CHEMISTRY 92, 449–459 (1991)

A Series of "Infinitely Adaptive Phases" in the Bi_2O_3–TeO_2 System

D. MERCURIO, B. H. PARRY, AND B. FRIT*

Laboratoire de Chimie Minérale Structurale, U.A.-C.N.R.S. No. 320, Université de Limoges, 123 Avenue A. Thomas, 87060 Limoges Cedex, France

AND G. HARBURN, R. P. WILLIAMS, AND R. J. D. TILLEY†

†*Department of Physics, and Division of Materials, University of Wales College of Cardiff, P.O. Box 917, Newport Road, Cardiff CF2 1XH, Great Britain*

Received October 1, 1990; in revised form February 8, 1991

An electron diffraction study of the intergrowth phases occuring in the composition range between Bi_2TeO_5 and $Bi_2Te_2O_7$ is reported. The complexity of the phase region is considerable and a large number of new superstructures have been found, many of which produce incommensurate diffraction patterns. The phases are composed of ordered intergrowths of Bi_2TeO_5- and $Bi_2Te_2O_7$-like units which evolve smoothly with composition across the existence range of these structures, approximately $1Bi_2O_3$:$1.35TeO_2$ to $1Bi_2O_3$:$1.85TeO_2$. It is proposed that the compounds conform to the description "infinitely adaptive phases."

I. Introduction

In two previous publications, Mercurio *et al.* (*1*) and El Farissi *et al.* (*2*) have reported on studies of the phases to be found in the composition region between Bi_2TeO_5 and $Bi_2Te_2O_7$ in the Bi_2O_3–TeO_2 system. These authors determined the structure of Bi_2TeO_5 and gathered enough information to propose an idealized model for the phase $Bi_2Te_2O_7$. These parent structures are both derived from a cubic fluorite type substructure of unit cell parameter a_F which contains ordered columns of Te atoms arranged so as to accommodate the lone pairs of electrons associated with the Te^{4+} state. The composition region between these two parent compounds contains a homologous series of phases of considerable complexity. The idealized structures of these phases, however, can be described as intergrowths of the two parent structures, as shown in Fig. 1.

As always with such regions of complex intergrowth, it is difficult to carry out phase analysis using classical powder X-ray diffraction techniques. It has therefore been necessary to turn to electron diffraction to elucidate this aspect of the composition range. In a preliminary study (*3*) we calculated the electron diffraction patterns expected from these types of phases and compared the results with experimentally

*To whom correspondence should be addressed.

0022-4596/91 $3.00

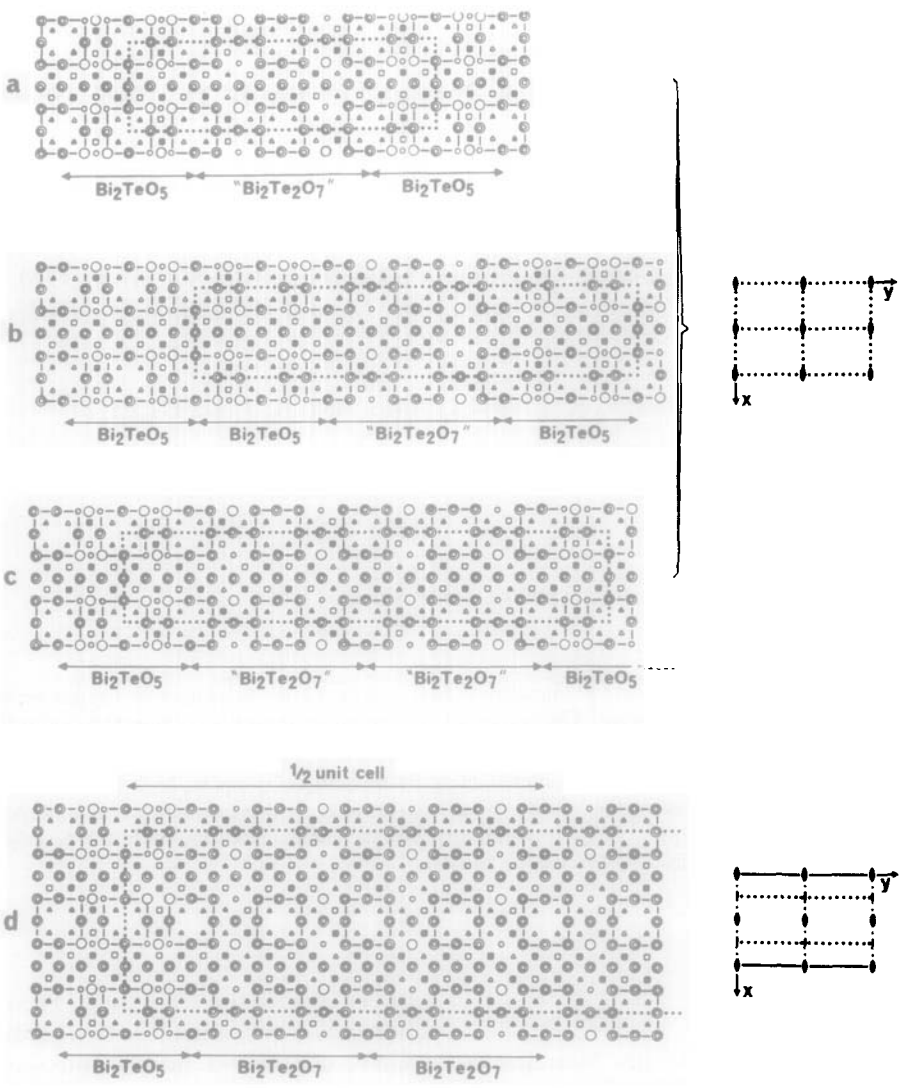

FIG. 1. Projections down (001) of the idealized structures of the intergrowths (a) $Bi_2TeO_5 + Bi_2Te_2O_7$, (b) $2Bi_2TeO_5 + Bi_2Te_2O_7$, (c) $Bi_2TeO_5 + 2Bi_2Te_2O_7$, (d) $Bi_2TeO_5 + 4Bi_2Te_2O_7$.

obtained patterns and with optical reconstructions of diffraction patterns expected from such intergrowths. In this paper we present a more complete study of the electron diffraction patterns and show that the composition range contains a large number of ordered phases of the type described by Anderson as "infinitely adaptive phases" (*4*). The diffraction patterns themselves can be interpreted as arising from ordered intergrowth of structural lamellae of thickness $3a_F$ and contiguous pairs of lamellae of thickness $4a_F$.

II. Experimental

The samples were prepared from high-purity α-Bi_2O_3 and TeO_2. The Bi_2O_3 was

initially heated at 550°C overnight in flowing oxygen. Immediately before use it was heated for a period of several hours at 800°C in air and checked by powder X-ray diffraction for phase purity. The TeO_2 was prepared from the decomposition of $Te(OH)_6$ which had been heated overnight in flowing oxygen at 550°C in a gold crucible. The reaction is

$$H_6TeO_6 \rightarrow TeO_2 + 3H_2O + \tfrac{1}{2}O_2.$$

Before use the TeO_2 was heated in air at 550°C for several hours in a gold crucible and checked for phase purity by X-ray diffraction. Appropriate weights of these samples of Bi_2O_3 and TeO_2 were ground together in an agate mortar and heated in sealed gold tubes for 16 hr. After heating, the tubes were quickly removed from the furnace and then allowed to cool in air. The compositions prepared and temperatures used are shown in Fig. 2.

After reaction, samples were checked by X-ray powder diffraction using a Guinier–de Wolff powder camera. For electron microscope examination, small quantities of samples were gently crushed in an agate mortar under *n*-butanol and a drop of the resultant suspension was allowed to dry on a holey carbon support film on a copper grid. Samples were examined in a Jeol 100B electron microscope operated at 100 kV and fitted with a top-entry stage capable of ±30° tilt, a Jeol 100C electron microscope fitted with a side-entry stage capable of ±60° tilt or a Jeol 200CX electron microscope operated at 200 KV and fitted with a top-entry stage capable of ±10° tilt. The compositions of some samples were determined with a Jeol 35CF scanning electron microscope fitted with an EDAX analysis system.

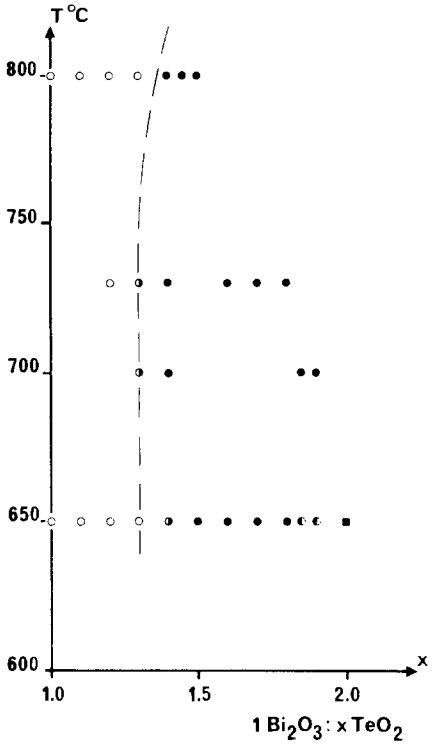

FIG. 2. Compositions $1Bi_2O_3$:$xTeO_2$ studied in the present investigation; ●, samples containing only intergrowth phases; ○, samples containing only a Bi_2TeO_5-type structure; ◑, samples containing both intergrowth phases and a Bi_2TeO_5-type structure; ◐, samples containing both intergrowth phases and $Bi_2Te_2O_7$; ■, samples containing only $Bi_2Te_2O_7$. The dotted lines represents tentative phase boundaries.

III. Results and Interpretation

The phase analysis resulting from the electron diffraction patterns is summarized in Fig. 2 and reported in Table I. These data show that for samples richest in Bi_2O_3, with $Bi_2O_3 : TeO_2$ ratios of 1 : 1.1, 1 : 1.2, and 1 : 1.3, only diffraction patterns similar to that of Bi_2TeO_5 were observed. In these, the b^* axis of the fluorite-type subcell was always divided into three by two equispaced superlattice spots, as shown in Fig. 3a. We tentatively interpret this as revealing the existence of a Bi_2TeO_5-like solid solution region which will be discussed in a future publication. Over the middle part of the composition range, diffraction patterns characteristic of the intergrowth phases were found. In samples prepared at 650°C,

TABLE I

ELECTRON MICROSCOPE PHASE ANALYSIS

$Bi_2O_3:xTeO_2$	Temperature (°C)	Experimental multiplicity l	No.	Mean l	SD $\sigma(l)$
1.0	800	3.0 only		3.0	
1.1	800	3.0 only		3.0	
1.2	800	3.0 only		3.0	
1.3	800	3.0 only		3.0	
1.4	800	23.6, 21.6, 23.0, 22.2 21.9, 22.2, 21.2, 21.6 24.7, 21.1, 21.8, 22.2 23.3	13	22.3	1.0
1.45	800	21.2, 20.4, 21.4, 21.5 19.6, 19.8, 20.8, 21.2	8	20.7	0.7
1.5[a]	800	19.2, 19.1, 19.4, 18.6 18.6, 18.6	6	18.9	0.4
1.5[a]	800	17.7, 18.9, 19.6, 18.9	4	18.8	0.8
1.2	730	3.0 only		3.0	
1.3	730	3.0, 3.0, 3.0, 3.0, 3.0	5	3.0	
		22.0, 21.8, 21.0, 22.3 22.3	5	21.9	0.5
1.4	730	19.7, 19.7, 20.0, 19.9 20.2, 19.9, 19.1, 19.1 19.5, 20.2	10	19.5	0.7
1.6	730	16.4*, 17.2, 16.1, 16.4 15.1, 15.7*, 15.1, 17.5 16.3	9	16.2	0.8
1.7	730	12.7*, 13.2, 12.8, 13.1 12.5	5	12.9	0.3
1.8	730	11.5, 11.3, 11.6, 11.9 11.6, 11.4, 11.8, 12.3	8	11.7	0.3
1.3	700	3.0, 3.0, 3.0, 3.0, 3.0 3.0	6	3.0	
		22.3, 22.1, 21.8, 21.7	4	22.0	0.2
1.4	700	21.2, 20.1, 19.3, 20.1 19.5, 19.5, 19.3	7	19.9	0.7
1.85	700	11.2, 11.0, 11.2, 10.9 11.1	5	11.1	0.1
1.9	700	10.8, 11.3, 11.6, 10.2 11.6	5	11.1	0.6
1.0	650	3.0 only		3.0	
1.1	650	3.0 only		3.0	
1.2	650	3.0 only		3.0	
1.3	650	3.0 only		3.0	
1.4	650	3.0, 3.0, 3.0, 3.0	4	3.0	
		15.8, 17.2, 17.7, 19.1 19.1*, 19.0*, 16.5	7	17.6	1.3
1.5	650	15.5, 18.0, 15.5, 15.8 14.6*, 15.4, 14.6, 15.7* 15.5*, 14.2*	10	15.5	1.0
1.6	650	13.9, 12.6, 13.3*,14.2 12.8, 13.2, 14.2*, 15.8* 13.5, 14.0, 13.0, 12.8	12	13.6	0.9

TABLE I—*Continued*

ELECTRON MICROSCOPE PHASE ANALYSIS

$Bi_2O_3 : xTeO_2$	Temperature (°C)	Experimental multiplicity l	No.	Mean l	SD $\sigma(l)$
1.7	650	12.0, 12.1, 12.0, 12.4 12.1, 11.7, 12.0, 12.0 11.6, 12.0, 12.0	11	12.0	0.2
1.8	650	10.4, 10.4*, 10.5, 10.5 11.1, 10.4, 11.0, 10.5 10.4, 10.4	10	10.6	0.3
1.85	650	11.7, 10.6, 11.9, 10.4 10.2, 10.4, 10.4, 9.9	8	10.7	0.7
		8.0, 8.0	2	8.0	
1.9	650	10.3, 10.3, 10.1, 10.5 9.9	5	10.2	0.2
		8.0, 8.0, 8.0, 8.0, 8.0, 8.0	6	8.0	
2.0	650	8.0 only		8.0	

Note. All patterns contained straight rows of superlattice spots except those marked by an asterisk which were tilted.

[a] Two different preparations.

crystal fragments with diffraction patterns identical to that expected from the phase $Bi_2Te_2O_7$ were observed to coexist with the intergrowth phases in the TeO_2-rich part of the composition range, revealing the existence of a narrow two-phase region under the preparation conditions used in this study.

The diffraction patterns from the intergrowth phases consisted of an almost square array of intense reflections which correspond to the {200} reflections expected from the fluorite substructure. Precise indexing leads to the conclusion that each section contained the b^* and c^* axes, i.e., the electron beam was parallel to [100]. No subdivision of the c^* direction was observed, in accordance with previous observations (*2, 3*). However, in the b^* direction, superlattice spots were always seen. The intensity of the superlattice reflections rose to a maximum at a point somewhere between $\frac{1}{4}$ and $\frac{1}{3}$ of d^*_{020} and between $\frac{2}{3}$ and $\frac{3}{4}$ of d^*_{020} as can be seen from the examples shown in Figs. 3b–3f. The quantity d^*_{020} is defined as the distance from the 000 to the 020 sublattice reflection. The number, spacings, and intensities of the superlattice reflections varied greatly. Generally, the rows of superlattice spots were strictly parallel to the b^* direction, but we draw attention to the fact that some diffraction patterns, summarized in Table I, were found in which the superlattice spots were at a small angle to this direction and hence showed an "orientation anomaly" (*5*). Despite the complexity, the superlattice spots were always sharp and no traces of diffuse scattering or streaking were ever detected.

In order to characterize the extent of the apparent unit cell in the direction parallel to the b axis, an experimental multiplicity, l, was determined. The quantity l is defined as the ratio d^*_{020}/d^*_{SL}, where d^*_{SL} is the separation of two adjacent superlattice reflections measured near to the maxima in intensity referred to above. The results are recorded in Table I and the average values of l are plotted as a function of composition in Fig. 4. This reveals that the superstruc-

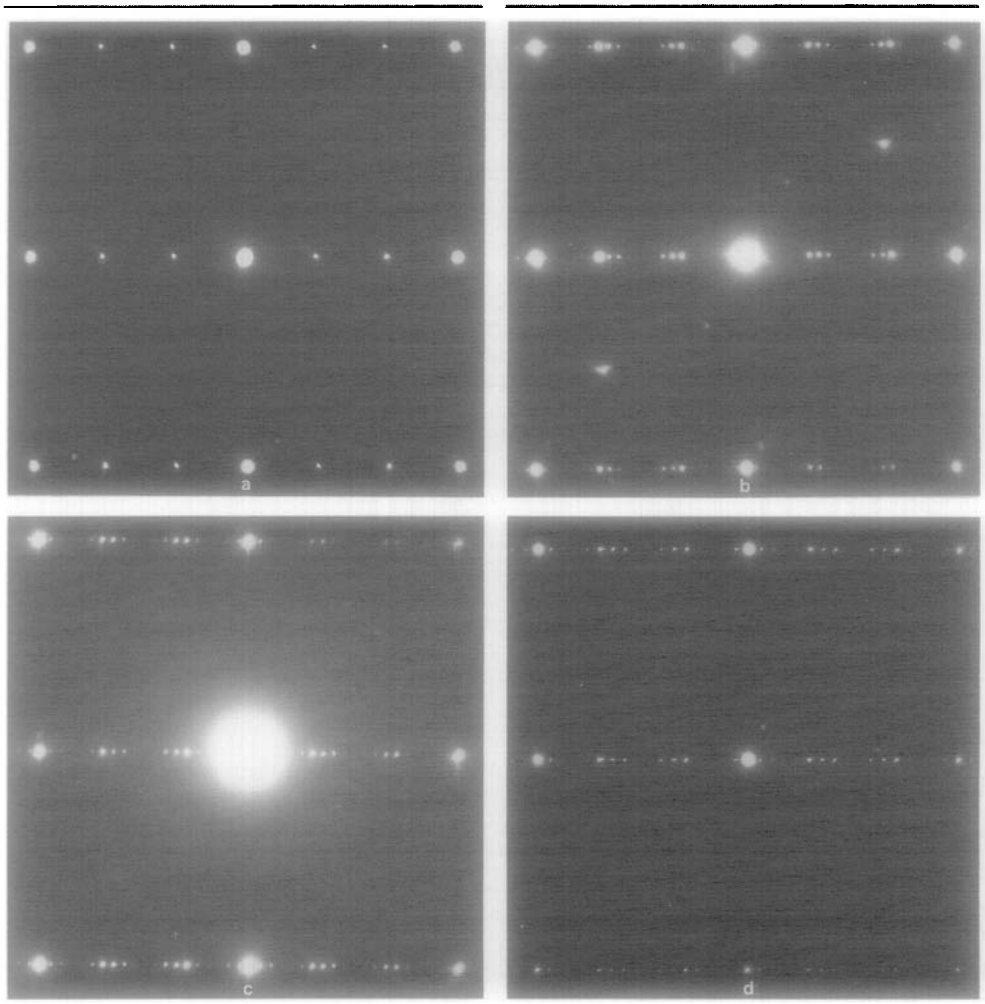

FIG. 3. Electron diffraction patterns from (a) $1Bi_2O_3:1TeO_2$ (Bi_2TeO_5), $l = 3$; (b) $1Bi_2O_3:1.4TeO_2$ prepared at a temperature of 800°C; (c) $1Bi_2O_3:1.5TeO_2$ (800°C); (d) $1Bi_2O_3:1.6TeO_2$ (730°C); (e) $1Bi_2O_3:1.7TeO_2$ (730°C); (f) $1Bi_2O_3:1.8TeO_2$ (730°C).

ture evolves both with composition and with the temperature at which the samples were prepared.

The values of l given in Table I indicate that the diffraction patterns were mostly incommensurate. This feature could sometimes be directly seen as "spacing anomalies" (*5*). These anomalies occur at three points between the fluorite subcell 000 and 020 reflections shown in the schematic example in Fig. 5. They are clearly visible on Figs. 3e and 3f and will be revealed by measurement on some of the other figures.

A detailed interpretation of the diffraction patterns involves the notation that we have previously established (*3*). Briefly, an intergrowth structure can be thought of as being built up from an ordered sequence of M blocks of $4a_F/2$ (half unit cells of $Bi_2Te_2O_7$) and N blocks of $3a_F/2$ (half unit cells of Bi_2TeO_5), which allows us to use the compact notation $\{4^M3^N\}$ for the stacking se-

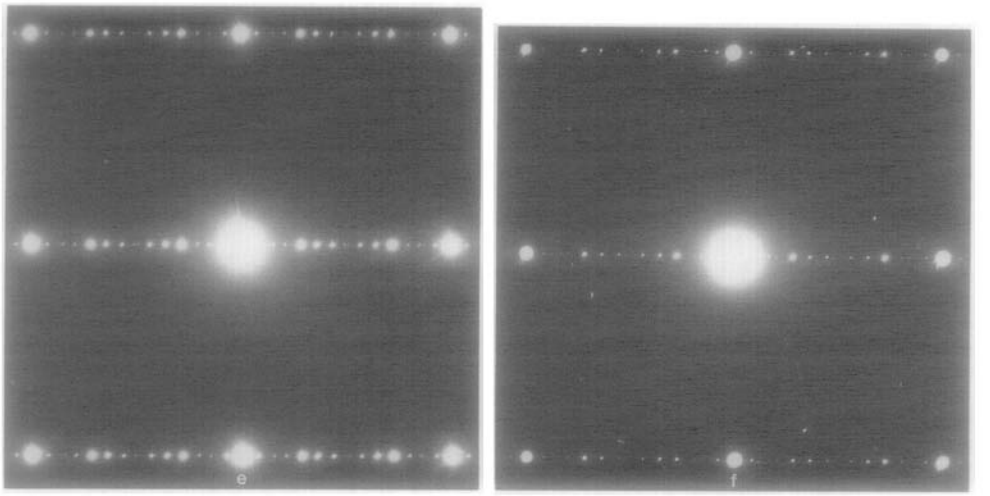

FIG. 3—*Continued*

quence in a given structure. The parameter L is defined as $(4M + 3N)$ and the stacking repeat distance is given by $L \cdot a_F/2$. Thus for the intergrowth of Bi_2TeO_5 and $Bi_2Te_2O_7$ shown in Fig. 1a, the stacking sequence is $\{4^23^2\}$, $L = 4M + 3N = 14$ and the stacking repeat distance is $14a_F/2$.

An overall consideration of the diffraction patterns obtained in this study suggested that despite the complexity found, only five base structures were present. In the samples with compositions closest to the Bi_2TeO_5 domain the number of superlattice spots lying between the 000 and 020 substructure reflections was ideally 22. Thereafter, the number of such superlattice spots contained in the same interval gradually diminished via ideal sequences of 19, 16, and 13 to 10 in samples close to $Bi_2Te_2O_7$ in composition.

This form of the diffraction patterns leads us to calculate the expected intensity variations for structures corresponding to L values and stacking sequences of 11, $\{4^23^1\}$; 14, $\{4^23^2\}$; 17, $\{4^23^3\}$; 20, $\{4^23^4\}$; and 23, $\{4^23^5\}$, using the same model to represent the intergrowth structures that was employed earlier (*3*). Briefly, this involves representing the structures by an array of δ-functions and

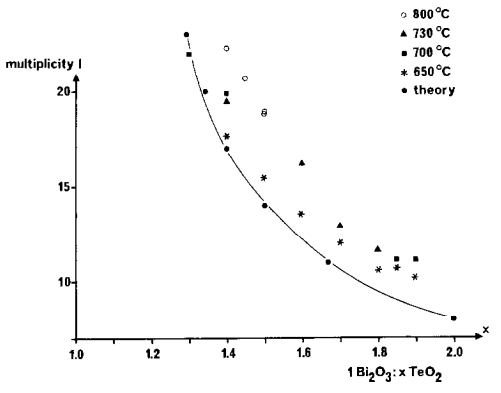

FIG. 4. The mean values of the experimental multiplicity, I, of the intergrowths found in the samples heated at 800, 730, 700, and 650°C as a function of the composition.

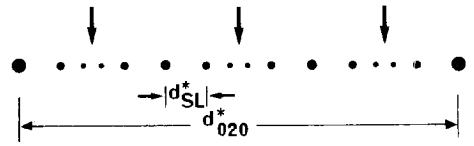

FIG. 5. Schematic illustration of the central line in an incommensurate diffraction pattern with the "spacing anomalies" arrowed.

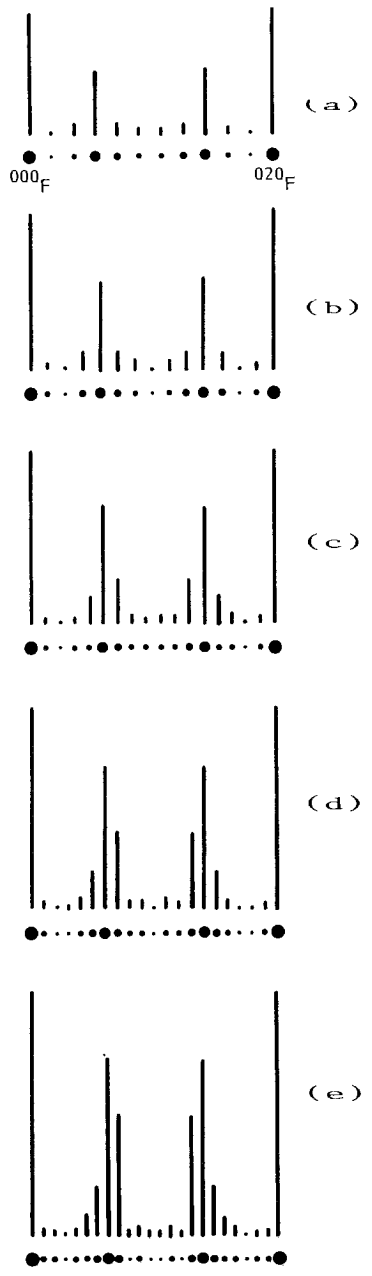

FIG. 6. Calculated intensities for the superlattice spots lying between the 000 and 020 subcell reflections for the sequences (a) $\{4^23^1\}$ (L = 11); (b) $\{4^23^2\}$ (L = 14); (c) $\{4^23^3\}$ (L = 17); (d) $\{4^23^4\}$ (L = 20); (e) $\{4^23^5\}$ (L = 23). In each part of the figure, the intensities of the reflections, represented as vertical lines, are shown above a schematic illustration of the distribution and intensities of the reflections.

evaluating the Fourier transform of the array. The expected intensities are derived directly from the Fourier transform, which is a representation of the Fraunhofer diffraction pattern of the array of δ-functions. The results are shown in Fig. 6. It is seen that the calculated diffraction patterns are commensurate, that the number of superlattice spots lying between the 000 and 020 subcell reflections follows the sequence 10, 13, 16, 19, and 22 and the number of superlattice spots lying between the two strongest superlattice spots follow the sequence 4, 5, 6, 7, and 8. These calculated patterns are in agreement with the experimental results and confirm that the overall features of the diffraction patterns can be explained assuming an intergrowth of blocks of {3} and {4} as proposed in (*2*) with base structures given by the sequence detailed above.

In order to interpret the incommensurate aspects of the diffraction patterns, consider the patterns shown in Figs. 3e and 3f. The incommensurate nature of the diffraction patterns is clearly revealed by the spacing anomalies visible at the center point between the fluorite subcell reflections. Measurement of the patterns gives the multiplicity l as (12.8 ± 0.2) for Fig. 3e and (12.3 ± 0.2) for Fig. 3f. These values of l lie between the commensurate L = 11 and L = 14 sequences.

A more quantitative analysis can be made following the procedure described by de Ridder *et al.* (*5*). The multiplicity, l, is not an integer in an incommensurate pattern, but can be expressed as a ratio p/q, where p and q are the smallest integers consistent with the precision of the data. The periodicity of the stacking, which is equal to $L \cdot a_F/2$, is given by $p \cdot d_{020}$ or $q \cdot d_{SL}$.

As an example we can consider the diffraction pattern shown in Fig. 3e. Following (*5*), the multiplicity l, 12.8, can be written as 128/10 or 64/5, whence L = 64 and the stacking repeat distance = $64d_{020} = 64a_F/2$. This corresponds to a sequence of three

units of 4^23^2 and two units of 4^23^1 to produce the stacking sequence $4^23^24^23^24^23^24^23^14^23^1$. The composition has moved slightly closer to TeO_2 by virtue of this substitution. It is also possible, of course, to find other sequences which fit the value of L found. We consider this further below. An identical procedure can be followed with Fig. 3f, leading to the conclusion that the stacking repeat distance is $123a_F/2$. This can be interpreted as being due to a number of possible repeat sequences, one of which is a sequence of eight units of 4^23^2 plus one unit of 4^23^1.

Obviously small changes in the measured value of l will lead to enormous differences in the value of L and hence in the length of the stacking sequence. However, even with modest values of L, such as that just calculated for Fig. 3f, the number of possibilities for the stacking sequence is large and it is not easy to determine if a chosen sequence is correct. For example the sequence suggested for Fig. 3f is not reasonable from a chemical point of view and a sequence with more equal numbers of units of 4^23^2 and 4^23^1 is to be preferred.

In order to clarify this aspect, calculations of intensity profiles were made in the same way as before for a sequence of structures lying between $L = 11$, i.e., $\{4^23^1\}$, and $L = 14$, i.e. $\{4^23^2\}$. The sequences $[7\times\{4^23^1\} + 1\times\{4^23^2\}]$, $[4\times\{4^23^1\} + 1\times\{4^23^2\}]$, $[2\times\{4^23^1\} + 1\times\{4^23^2\}]$, $[1\times\{4^23^1\} + 2\times\{4^23^2\}]$, $[1\times\{4^23^1\} + 4\times\{4^23^2\}]$, and $[1\times\{4^23^1\} + 7\times\{4^23^2\}]$ were chosen to give an overall impression of the way in which the diffraction patterns evolve between these limits. The results are displayed in Fig. 7. The evolution of the patterns can be best seen by viewing the figure at a glancing angle. It is apparent that Figs. 3e and 3f are well represented by the simulations shown as Figs. 7d and 7c, respectively. Stacking sequences appropriate to the relative amounts of the end structures present can be estimated from this figure.

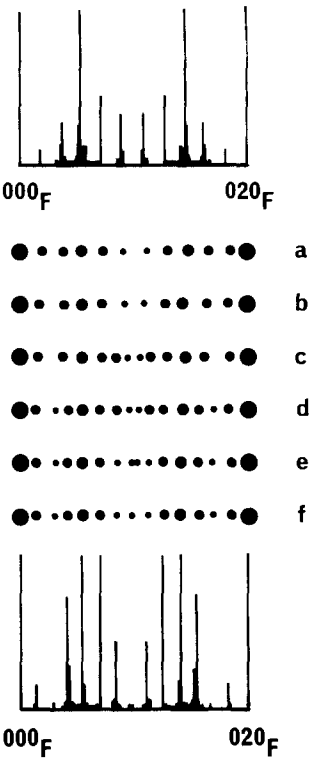

FIG. 7. Calculated intensities for the superlattice spots lying between the subcell 000 and 020 reflections for structures lying between $L = 11$ $\{4^23^1\}$ and $L = 14$ $\{4^23^2\}$. (a) $[7\times\{4^23^1\} + 1\times\{4^23^2\}]$; (b) $[4\times\{4^23^1\} + 1\times\{4^23^2\}]$; (c) $[2\times\{4^23^1\} + 1\times\{4^23^2\}]$; (d) $[1\times\{4^23^1\} + 2\times\{4^23^2\}]$; (e) $[1\times\{4^23^1\} + 4\times\{4^23^2\}]$; (f) $[1\times\{4^23^1\} + 7\times\{4^23^2\}]$. In (a) and (f) both the intensities, represented as in Fig. 6 and a schematic illustration of the positions and intensities of the reflections are given, while in (b) to (e) only the schematic reflections are shown. The evolution of the patterns is best seen by viewing the figure at grazing incidence.

Discussion

The phase analysis via electron diffraction is in good agreement with that described previously, derived from X-ray diffraction (*2*). In the present study, the results indicate that superstructures begin to form at compositions of about $1Bi_2O_3 : 1.3TeO_2$. The superstructures evolve smoothly with composition to approximately $1Bi_2O_3 : 1.85TeO_2$.

In the intergrowth composition region the composition variation is accommodated by ordered deletions or insertions of units of {3} in a base structure, which appears to be one of five types represented by L values of 11, 14, 17, 20, and 23. The fact that there is no great change in the nature of the diffraction patterns after a composition of $1Bi_2O_3 : 1.85TeO_2$ for samples heated at 650°C suggests that a second phase boundary may exist near this point. However, the data in Table I and Fig. 4 show that the value of the multiplicity, l, found in this region falls as the temperature decreases. It is therefore possible that at lower temperatures the gap between $L = 8$ and $L = 11$ will be bridged and a continuum of phases occur, with an absence of a phase boundary.

Although the analysis for the evolution of the intergrowth phases described above is correct in principle, it does not account for two important observations. The value of l found in any sample was higher than that predicted by a simple intergrowth of units of composition Bi_2TeO_5 and units of composition $Bi_2Te_2O_7$. Moreover, the value of l increased as the temperature of sample preparation increased. For example, a 1 : 1 intergrowth between Bi_2TeO_5 and $Bi_2Te_2O_7$, corresponding to $L = 14$, $\{4^23^2\}$, should occur at a composition of $1Bi_2O_3 : 1.5TeO_2$, i.e., $MO_{1.7143}$. From an examination of Fig. 4, it is apparent that the samples prepared at this composition have mean l values of 15.5 at 650°C and 18.9 at 800°C. In all of the samples investigated, the l value recorded was greater than that expected from a simple intergrowth of parent phases of compositions Bi_2TeO_5 and $Bi_2Te_2O_7$, which seems to indicate that all the samples contained less TeO_2 than calculated.

An explanation can be found when the extent of the solid solution region at the Bi_2TeO_5 end of the phase range is considered. According to electron microscope results, the Bi_2TeO_5 phase persists up to a composition of about $1Bi_2O_3 : 1.35TeO_2$, i.e. $MO_{1.7015}$, at a temperature of 800°C. Thus some of the TeO_2 is being incorporated into the Bi_2TeO_5 blocks and the number of blocks of type {4} which can contribute to the intergrowth decreases. The domain of the Bi_2TeO_5 solid solution appears to increase with temperature, which would be consistent with an increase of the apparent value of l with increasing temperature of sample preparation. The intergrowth phases are now regarded as made up of intergrowths between the 4^2 structure of composition $Bi_2Te_2O_7$ and a 3^2 structure which is a solid solution with a temperature variable composition.

To illustrate this, at 730°C, the solid solution range seems to be from Bi_2TeO_5 to about $1Bi_2O_3 : 1.35TeO_2$. A 1 : 1 intergrowth between 4^2 and 3^2 would have the composition $1Bi_2O_3 : 1.67TeO_2$, i.e. $MO_{1.7276}$. This is in agreement with the results presented in Fig. 4 within the precision of our measurements. The results also suggest that the extent of this solid solution becomes smaller as the temperature decreases so that preparations at 600°C may yield l values close to that calculated from the ideal model. Similarly at higher temperatures, it is possible that the Bi_2TeO_5 region may extend further across the composition range and no intergrowth structures may form.

The diffraction patterns obtained in this study were all, without exception, well ordered. Indications of disorder such as diffuse scattering or streaking, which are readily observed by electron diffraction, were never recorded in these experiments. This strongly suggests that every composition prepared is capable of producing its own ordered structure and that any composition whatsoever can be integrated into the crystal structure by the same method outlined above. The phases conform to the description "infinitely adaptive phases" given by J. S. Anderson (*4*).

Despite this observation, the fact that only five underlying structure types exist

raises the question of whether, if samples were heated for longer periods of time, the intergrowth phases would segregate into these structures alone. That is, classical two-phase regions may occur between $L = 11$ and $L = 14$, $L = 14$ and $L = 17$ and so on, instead of the continuum observed in the present experiments. Examination of samples heated for longer periods of time is therefore of some interest. Further experiments are also needed to clarify the conditions under which the diffraction patterns which showed noncollinear or "tilted" rows of superlattice spots are produced. Moreover, the mechanisms by which these intergrowths achieve order over large unit cells are not yet understood. Finally, we draw attention to the simple nature of the model used to simulate the diffraction patterns. Clearly, refinement of this model is needed to encompass more crystallographic detail. These points will be addressed in future publications.

Acknowledgments

R.J.D.T. is indebted to the University of Limoges and B.H.P. to the Royal Society for financial assistance which has made this collaborative study possible.

References

1. D. Mercurio, M. El Farissi, B. Frit, and P. Goursat, *Mater. Chem. Phys.* **9,** 467 (1983).
2. M. El Farissi, D. Mercurio, and B. Frit, *Mater. Chem. Phys.* **16,** 133 (1987).
3. D. Mercurio, B. Frit, G. Harburn, B. H. Parry, R. P. Williams, and R. J. D. Tilley, *Phys. Status Solidi A* **108,** 111 (1988).
4. J. S. Anderson, *J. Chem. Soc. Dalton Trans.*, 1107 (1973).
5. R. de Ridder, J. van Landuyt, and S. Amelinckx, *Phys. Status Solidi A* **9,** 551 (1972).